

The Preparation and Electrochemical Performance of Nitrogen-doped Graphene/Co(OH)₂ Composite

Yunshan Bai^{1,2,*}, Lude Lu², Jianchun Bao², Guoxiang Sun¹, Beibei Zhang¹,
Jianping Zeng¹, Song Chen^{1,*}

¹ College of Chemistry and Chemical Engineering, Yancheng Institute of Technology, Yancheng 224003, P. R. China

² Key Laboratory for Soft Chemistry and Functional Materials of Ministry of Education, Nanjing University of Science and Technology, Nanjing 210094, P. R. China

*E-mail: ysbai_njust@163.com, 15005101586@163.com

Received: 30 August 2018/ Accepted: 28 October 2018 / Published: 30 November 2018

There are certain defects in the graphene prepared by redox method. These defects can cause a decrease in the electrochemical performance of the resulting grapheme. The performance of chemically prepared graphene can be improved to some extent by the doping of heteroatoms. In this paper, the electrochemical performance of graphene-based composites is improved by doping with nitrogen. The results show that the electrochemical performance of the nitrogen-doped graphene-based composite as electrode material is better than that of the undoped graphene-based composite as electrode material. The Nitrogen doped graphene/Co(OH)₂ composite electrode material was prepared by one-step method. Urea played an important role in the synthesis process. During the reduction of graphene oxide, in-situ nitrogen doping happened simultaneously. The slow decomposition of urea provided the desired OH⁻ for the formation of Co(OH)₂ and regulated its growth rate. Meanwhile, the excess CO₂, OH⁻ and NH₃ acted as soft templating agents for Co(OH)₂ to control their growth to obtain morphology-specific composites.

Keywords: graphene based composites, electrode materials, supercapacitor, electrochemical performance, doped graphene

1. INTRODUCTION

Graphene is widely used in the research area of supercapacitor electrode materials, mainly due to their excellent electrical and mechanical properties [1-7]. Graphene can be used as a supercapacitor and the main energy storage mechanism is based on the electric double layer [8]. The electrode material based on this mechanism has excellent cycle performance. However, its specific capacitance is far from the practical demand. Loading pseudo capacitance material on graphene (For example, Cobalt

Hydroxide, whose theoretical specific capacitance is about 3460 Fg^{-1} ; Nickel Hydroxide, whose theoretical specific capacitance is about 2358 Fg^{-1}) can increase the specific capacitance of electrode materials [9, 10]. Additionally, graphene-based composite materials used as supercapacitor electrode materials are often prepared by chemical methods (oxidation-reduction) [11-13]. The graphene obtained in this method has large defects, resulting the reduction of the excellent performance of graphene. This defect can be improved by loading with conducting polymer, and the performance of the graphene-based composite electrode material can also be improved by doping [14-16]. Nitrogen doping is an effective way to improve the performance of graphene prepared by chemical methods. The introduction of nitrogen atoms can form n-type semiconductors, thereby improving the electrical properties of chemically prepared graphene.

In this article, Nitrogen-doped Graphene/ Co(OH)_2 Composite was prepared by one-step method. Urea plays a key role in the reaction: 1) a reducing agent for graphene oxide; 2) a nitrogen source for nitrogen-doped graphene; and 3) a precipitant for Co(OH)_2 . The Co(OH)_2 nanowires were uniformly loaded on nitrogen-doped graphene sheets with the cooperational effects of excess urea and graphene. Nitrogen-doped graphene/ Co(OH)_2 composites showed better electrochemical performance than graphene/ Co(OH)_2 and pure Co(OH)_2 .

2. EXPERIMENTS

2.1. Reagents

Graphene oxide (lab made); cobalt nitrate ($\text{Co(NO}_3)_2$, AR, Shanghai Lingfeng Chemical Reagent Co., Ltd.); urea ($\text{CO (NH}_2)_2$, AR, Sinopharm Chemical Reagent Co., Ltd.); sodium hydroxide (NaOH), AR, Nanjing Chemical Reagent Co., Ltd.); deionized water (Ultrapure Milli-Q ultrapure water from the United States); Hg/HgO electrode.

2.2 Preparation of graphene oxide by two-step method [17, 18]

1) In the first step, 20 g of graphite (12500 mesh) was weighed and added into a mixture containing 30 mL of concentrated sulfuric acid, 10 g of potassium persulfate, and 10 g of phosphorus pentoxide mixture and the reaction was kept at $80 \text{ }^\circ\text{C}$ for 8 hours; After the reaction was completed, it was filtered and washed until the pH of the filtrate was 7; Then, it was set overnight.

2) The pre-oxidized graphite was added to 460 mL of concentrated sulfuric acid; 60 g of potassium permanganate was added into the above solution, and the speed of addition was controlled so that the temperature does not exceed $20 \text{ }^\circ\text{C}$; after the addition was completed, the mixture was heated to $35 \text{ }^\circ\text{C}$. The mixture was stirred for 2 hours. Then, 920 mL of ultrapure water was slowly added, and the controller temperature was $95\text{-}100 \text{ }^\circ\text{C}$, maintaining this temperature for 30 minutes. The experiment was terminated by the addition of 2.8 L of water and 50 mL of 30% hydrogen peroxide. After the reaction was completed, it was filtered and washed with 5 L hydrochloric acid solution (1:10 (by volume)) to obtain graphene oxide.

2.3 Preparation of Nitrogen-doped Graphene/ $\text{Co}(\text{OH})_2$ Composite

In this process, 100 mg of graphene oxide was ultrasonically dispersed in 100 mL of aqueous solution to obtain 1 mg mL^{-1} of graphene oxide aqueous solution. Then, 1.84 g of cobalt nitrate was added to the above graphene oxide solution, and after stirring for 30 min in a three-necked flask, 18 g of urea was added and stirred for 1 hour, and then heated to 95°C . After 12 hours of reaction, it was filtered and washed with a large amount of deionized water. The experiment is illustrated in Figure 1. The obtained nitrogen-doped graphene/ $\text{Co}(\text{OH})_2$ is noted as NGE-Co.

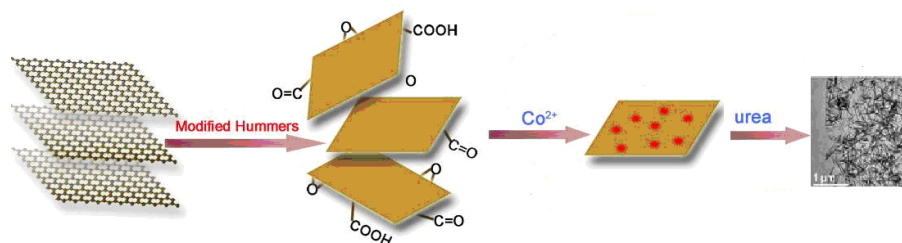


Figure 1. Illustration for the synthesis process of nitrogen-doped graphene/ $\text{Co}(\text{OH})_2$ composite

As a comparison, pure $\text{Co}(\text{OH})_2$ and graphene/ $\text{Co}(\text{OH})_2$ Composite were prepared. When graphene/ $\text{Co}(\text{OH})_2$ was prepared, NaOH was used as a reducing agent for graphene oxide and the precipitant of $\text{Co}(\text{OH})_2$ [19].

2.4 Characterization methods

Morphological characterization: The test instrument was X-ray energy spectroscopy (EDS) transmission electron microscope (JEOL, Japan). The accelerating voltage was 200KV. During the preparation of the samples, the synthesized sample was ultrasonically dispersed in ethanol solution, and then dropped on the carbon support film. The scanning electron microscope was HITACHI S-4800.

Raman spectroscopy: The test instrument was British Renishaw Invia laser Raman spectrometer. The laser wavelength for testing was 514.5 nm, and the test range was $100\sim 4000 \text{ cm}^{-1}$.

XRD pattern: The test instrument was German Bruker Vector 22X-ray powder diffractometer. The test condition was in $\text{CuK}\alpha$ target position ($\lambda=1.5406 \text{ \AA}$), and the test range was $5 \sim 80^\circ$.

XPS elemental analysis: The test instrument was Japanese PHI Quantera II X-ray photoelectron spectroscopy and the excitation source was C_{60} .

TGA test: The test instrument was Mettler-Toledo TGA/SDTA851. The test condition was $20 \sim 500^\circ\text{C}$, and the heating rate is 5°C min^{-1} .

2.5 Electrode preparation and performance testing

A three-electrode system was used. A platinum plate electrode was used as a counter electrode and a saturated calomel electrode was used as a reference electrode. The working electrode was prepared in the lab.

Working electrode preparation process: Foamed nickel was used as the current collector. Before use, it was ultrasonically cleaned for 3 times with ethanol and ultrapure water and dried for weighing. According to the mass ratio of 85:10:5, a certain amount of sample. Conductive Carbon blacks and bonding agent were weighed. After thoroughly mixed, it was applied evenly onto the foamed nickel and the application area was controlled to be 1 cm^2 . After vacuum drying at $60 \text{ }^\circ\text{C}$, it was compacted (10 MPa) and weighed[20].

Electrochemical test: The test electrolyte was 6 mol L^{-1} of KOH. The test temperature was $22 \text{ }^\circ\text{C}$. The cyclic voltammetry and AC impedance test were conducted on CHI760C. The cyclic voltammetry test range was $-0.1 \sim 0.5 \text{ V}$. The AC impedance test frequency was from 1×10^5 to $1 \times 10^{-2} \text{ Hz}$. The test voltage was 0 V , and the amplitude was 5 mV . The constant current charge and discharge were tested in the Land, and the current densities were 0.2 A g^{-1} , 0.4 A g^{-1} and 0.8 A g^{-1} .

3. RESULTS AND DISCUSSION

3.1 Structural Characterization of Nitrogen-doped Graphene/ $\text{Co}(\text{OH})_2$ Composite

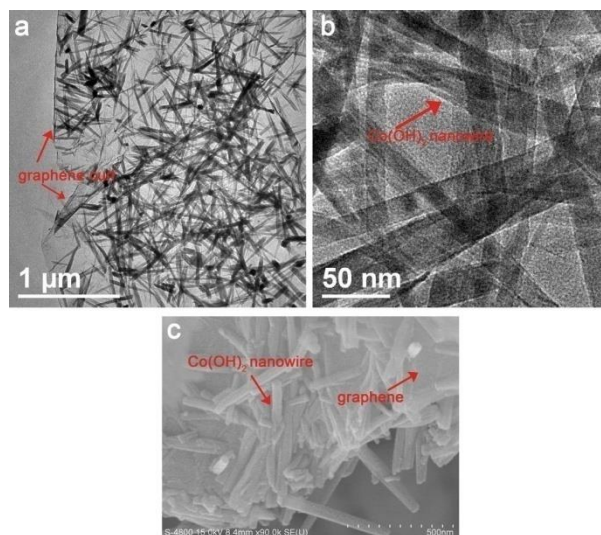


Figure 2. (a, b) TEM of NGE-Co and (c) SEM images of NGE-Co

The low-resolution and high-resolution TEM images of NGE-Co are shown in Figures 2a and 2b. As shown, a nanowire of cobalt hydroxide with a width of 40 nm and a length of several hundred nanometers was supported on the surface of graphene. In Fig. 2a, the curl of the graphene sheet and its low resolution with the carbon support film can be seen, indicating that the composite graphene (several layers) was obtained. The scanning electron micrograph of NGE-Co shows that the length of the cobalt hydroxide nanowire is about 500 nm .

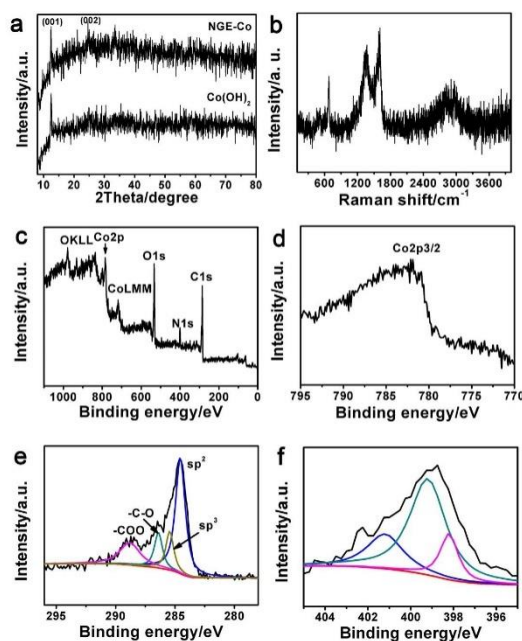


Figure 3. (a) XRD patterns of NGE-Co and Co(OH)_2 ; (b) Raman spectrum of NGE-Co; (c) XPS survey spectrum; Core-level XPS spectra of NGE-Co for (d) Co 2p_{3/2}, (e) C 1s, and (f) N 1s.

The XRD pattern of NGE-Co and pure cobalt hydroxide was shown in Figure 3a. The characteristic peaks of cobalt hydroxide are present in both NGE-Co and pure cobalt hydroxide, corresponding to P/3m1 hexagonal cobalt hydroxide (PDF#74-1057), which is consistent with previously reported literature [21, 22]. At the same time, there is no other crystal form of cobalt hydroxide shown in the pattern, indicating that a pure composite material was obtained. The peaks of 12.5° and 24.5° correspond to the (001) and (002) crystal planes under the crystal form. Compared with other crystal planes, the peaks at these two points are much larger than those of other peaks, which indicate that the cobalt hydroxide nanowires grew along the (00 ℓ) plane. The Raman spectrum of NGE-Co is shown in Figure 3b. The peak of 676 cm^{-1} is the vibration peak of E_g of cobalt hydroxide; the peak of 547 cm^{-1} is the vibration peak of A_{1g} of cobalt hydroxide; the peak of 445 cm^{-1} is the vibrational peak of O-Co-O [23, 24]. The D and G peaks of graphene in the composite are appeared at 1366 cm^{-1} and 1608 cm^{-1} , respectively, and the intensity ratio of the two peaks is 0.84, indicating that the structure of graphene oxide is no further destroyed during the reduction doping process. Figure 3c shows the XPS full spectrum of NGE-Co, which shows that the composite contains C, N, O, Co, and their contents are 39.9%, 10.2%, 6.9%, 13%, respectively. The peak of Co2p_{3/2} appears at 781.8 eV in Figure 3d, which is the characteristic peak of cobalt hydroxide [25]. Figure 3e shows the C1s spectrum of NGE-Co. The reduction of the content of oxygen-containing functional groups indicates that the graphene oxide was well reduced. The N1s spectrum shows that nitrogen was present in graphene in the form of graphitic nitrogen, pyrrole carbon and pyridinium, which means that nitrogen was doped into the composite.

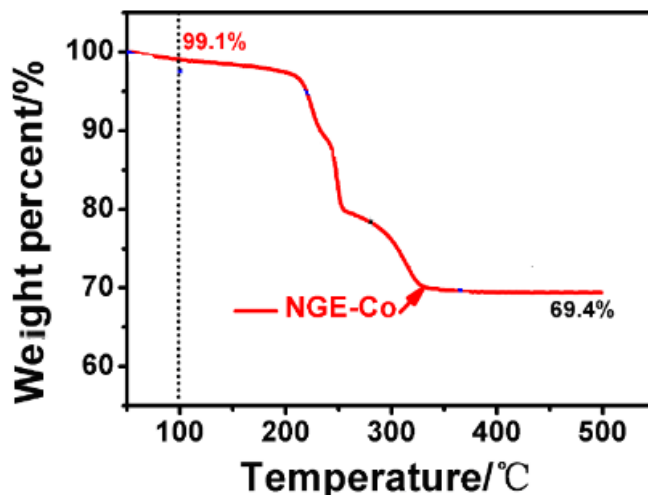


Figure 4. TG curve of NGE-Co

The content of each component of the nitrogen-doped graphene composite was further analyzed by thermogravimetry and the result was shown in Figure 4. It was reported in the literature that in the air after 400 °C, graphene will completely react, while Co(OH)_2 will be decomposed into CoO [26]. As shown in Fig. 4, after 450 °C, the TG curve of the composite tends to be stable, and the quality is no further reduced, indicating that the nitrogen-doped graphene composite was converted into the corresponding oxide. After 500 °C, the composite of nitrogen-doped graphene has 69.4% (NGE-Co), and the content of graphene in the three nitrogen-doped graphene composites is calculated to be 26.7% (NGE- Co).

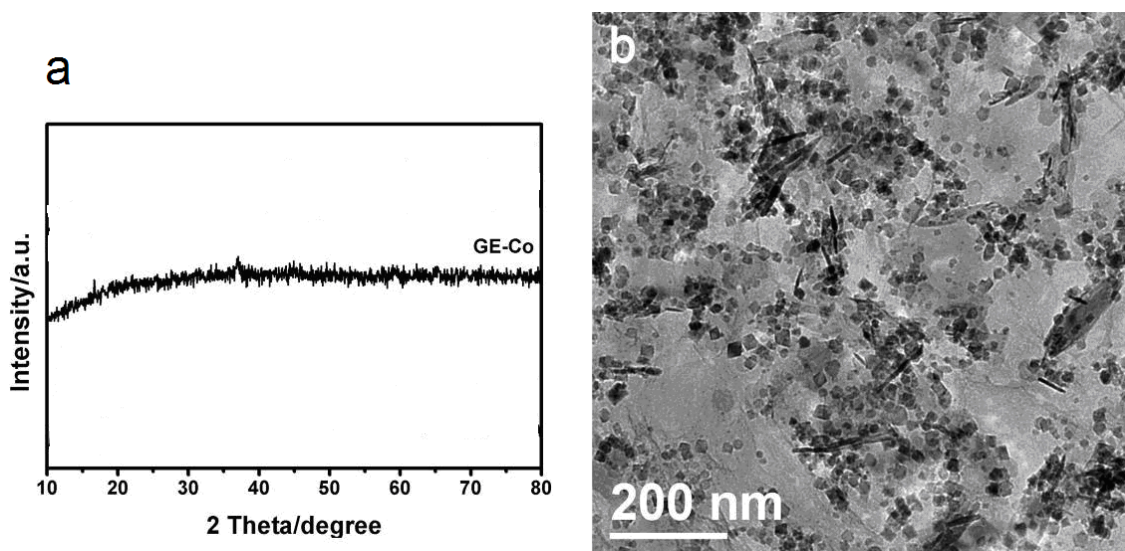
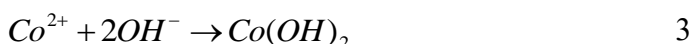
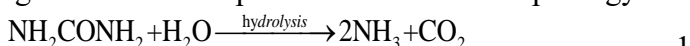


Figure 5. (a) The XRD patterns of GE-Co, and (b) the TEM images of GE-Co.

The XRD pattern of graphene/ Co(OH)_2 is shown in Figure 5a, and the TEM electron micrograph of graphene/ Co(OH)_2 is shown in Figure 5b. Figure 5b shows that cobalt hydroxide is supported on the

surface of graphene with square nanoparticles. From the above results, it can be seen that the morphology of the graphene/Co(OH)₂ composite prepared by using sodium hydroxide as a precipitant and the shape of nitrogen-doped graphene/Co(OH)₂ prepared by using urea as a precipitant are completely inconsistent, which indicates that urea plays a key role in the synthesis process. The reaction process is shown in Equations 1-3. Metal ions were adsorbed onto the surface of graphene oxide by acting on an oxygen-containing group on the graphene oxide. With heating to 95 °C, urea gradually decomposed to form OH⁻, acting as a precipitant for the formation of Co(OH)₂ and reducing the graphene oxide. At the same time, urea can also be used as a dopant to nitrogen doping graphene. Compared with sodium hydroxide, urea can slowly provide the generation of OH⁻ to better control the growth of hydroxide. Finally, under the action of graphene and excessive decomposition substances (OH⁻, NH₄⁺, CO₂), it grows into a composite with certain morphology.



3.2 Electrochemical Performance of Nitrogen-doped Graphene/Co(OH)₂ Composite

Cyclic voltammetry was used to test the storage behavior of nitrogen-doped graphene composites. Figure 6a is a cyclic voltammogram of NGE-Co at different sweep rates and GE-Co and single-component materials were tested under the same test conditions as a control, shown in Figure 6b.

Figures 6a and 6b show the cyclic voltammetry curves of NGE-Co, GE-Co and pure cobalt hydroxide. Compared with pure cobalt hydroxide, the cyclic voltammetry curve of NGE-Co has a larger rectangular frame, and the cyclic voltammetry curve of pure cobalt hydroxide has a pair of reversible redox peaks at 0.11V and 0.27V. The peaks are located at 0.08V and 0.19 V for NGE-Co, respectively. Compared with pure cobalt hydroxide, the potential difference of the redox peak of NGE-Co is 0.11 V, which is smaller than that of the pure cobalt hydroxide.

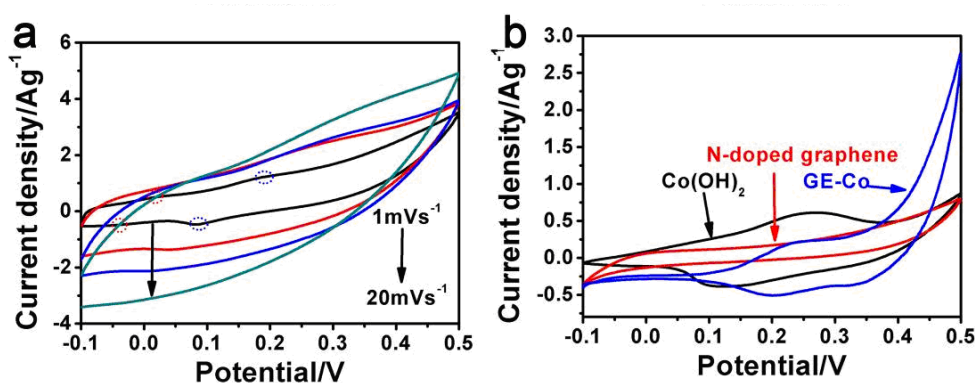
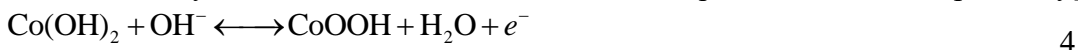


Figure 6.(a) The CV curves of NGE-Co in the scan rates of 1 mV s⁻¹, 5 mV s⁻¹, 10 mV s⁻¹, 20 mV s⁻¹; (b) the CV curves of Co(OH)₂, GE-Co and N-doped graphene/Co(OH)₂ at 1 mV s⁻¹.

Thus the reversibility of the electrode material increased after composition. In addition, the cyclic voltammetry curve of NGE-Co has one more pair of redox peaks (-0.04/0.02V) than pure cobalt hydroxide. According to the literature, the two pairs of redox peaks of NGE-Co correspond to the conversion of cobalt hydroxide in the electrodematerials of Equations 4 and 5, respectively[27].



At the same time, the potential difference between each pair of redox peaks indicates the reversibility of redox [31].

Figure 6a is a cyclic voltammetry curve for the composite of nitrogen-doped graphene/Co(OH)₂ at different sweep rates. The cyclic voltammogram of Figure 6a has a pair of reversible redox peaks at 0.08/0.19 V. The peak position does not change significantly with the sweep rate, indicating that NGE-Co had redox reaction with good reversibility[28, 29]. The shape of the CV curves are close to rectangle indicating a good capacitance behaviour of the composites (NGE-Co) and it also shows a distorted rectangular shape with redox peaks. As the sweep rate increases, the redox peaks move to both ends, and the peak current increases significantly, indicating that the capacitance of NGE-Co (in 6 mol L⁻¹ KOH solution) is composed of electric double layer capacitance and Faraday quasi-capacitance. Under low-sweep speed, the capacitance is dominated by electric double-layer capacitors, and under high-sweep speed, the capacitance is dominated by Faraday quasi-capacitors [38, 39].

As the sweep speed increases, the current response in the cyclic voltammetry curve increases rapidly. At the same time, when the sweep speed reaches 20 mV s⁻¹, the shape of the cyclic voltammetry curve remains unchanged, indicating that the material has better magnification characteristics. The excellent electrochemical performance of the nitrogen-doped graphene-based electrode material indicates that the introduction of nitrogen-doped graphene helps to improve the electrochemical performance of the electrode material. By calculation, with a sweep rate of 1 mV s⁻¹, the specific capacitance of the nitrogen-doped graphene-based composite material is 1040 F g⁻¹ (NGE-Co) and the specific capacitance of the graphene-based composite material is 885 F g⁻¹ (GE-Co), while the specific capacitance of pure Co(OH)₂ is 197 F g⁻¹ (Co(OH)₂). The specific capacitance of nitrogen-doped graphene under the same test conditions is 205 F g⁻¹ (-0.1V~0.5V).

It has been shown in the reference that the electrochemical performances of nitrogen-doped graphene/Co(OH)₂ composites are far superior to those reported for other N-doped carbon materials, including nitrogen/sulfur co-doped and hierarchical porous graphene hydrogels (251 F g⁻¹, 0.5 A g⁻¹) [33], N-doped graphene (312 F g⁻¹, 0.1 A g⁻¹) [34], p-phenylenediamine functionalized rGO (316 F g⁻¹, 0.5 A g⁻¹) [35], butane-1,4-diamine/rGO (119 F g⁻¹, 1A g⁻¹) [36], N-doped rGO(reduced graphene oxide) (390 F g⁻¹, 0.5 A A g⁻¹) [37]. It has similar electrochemical performance with Nitrogen-doped graphene (V₂O₅/NG)(1032.6F g⁻¹, 1 mVs⁻¹)[38]

Compared with pure Co(OH)₂, the electrochemical specific capacitance of graphene/Co(OH)₂ is increased, mainly because the introduction of reduced graphene oxide is beneficial to the dispersion of Co(OH)₂ and its good electrical conductivity. However, compared with pure Co(OH)₂ and graphene/Co(OH)₂, nitrogen-doped graphene/Co(OH)₂ has more excellent electrochemical properties, mainly because: 1) Nitrogen-doped graphene has better conductivity and capacitance characteristics than

reduced graphene[32]; 2) Dispersed nitrogen-doped graphene not only provides a large area in contact with the electrolyte, but also provides a large active area for the charge transport of the redox reaction; 3) The slow formation of OH^- affects the growth of the surface of $\text{Co}(\text{OH})_2$ on graphene; 4) $\text{Co}(\text{OH})_2$ exhibits better electrochemical performance with the help of nitrogen-doped graphene.

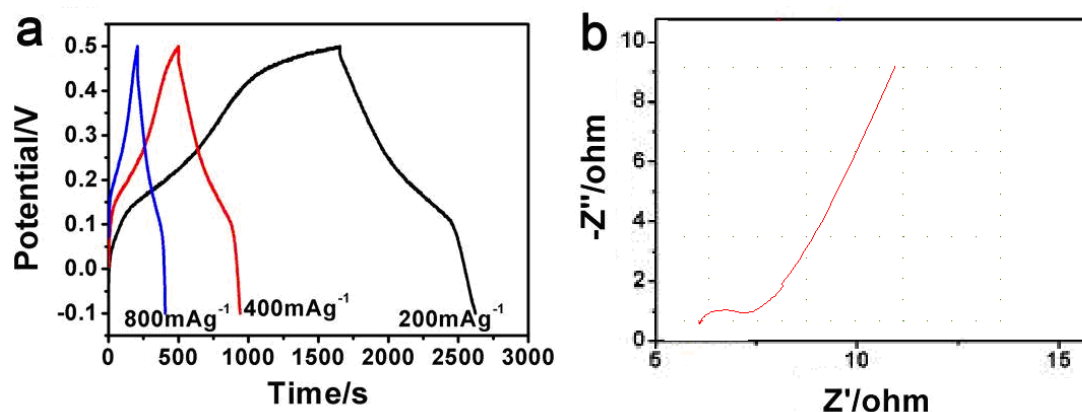


Figure 7. (a) The galvanostatic charge-discharge curves of NGE-Co at different current densities of 200 mA g^{-1} , 400 mA g^{-1} and 800 mA g^{-1} ; (b) EIS

Figure 7 shows the charge and discharge curves of nitrogen-doped graphene/ $\text{Co}(\text{OH})_2$ at different current densities. As shown, all the charge and discharge curves show different voltage platforms, indicating that the electrochemical capacitance of the nitrogen-doped graphene composites has different storage energy modes to store energy. At a current density of 200 mA g^{-1} , the specific capacitance of nitrogen-doped graphene is 350 F g^{-1} (NGE-Co), where their values are lower than the values reported in the literature. This is mainly because the content of hydroxide in the nitrogen-doped graphene composite is less, and the contribution of pseudocapacitor is less. When the current density rises to 400 mA g^{-1} , the specific capacitance of the nitrogen-doped graphene composite is about 91% (NGE-Co), indicating that these electrode materials have good magnification characteristics.

The AC impedance test range is from 10^{-2} Hz to 10^5 Hz, and its spectrum is shown in Figure 7b. The AC curve of nitrogen-doped graphene/ $\text{Co}(\text{OH})_2$ contains three parts: 1) a semi-arc with a deformation in the high-frequency region; 2) The intermediate frequency region has a 45° straight line; 3) There is a straight line with a larger slope in the low frequency region, and the straight line shows the capacitance performance of the electrode material. The starting point of the AC impedance is the contact impedance, and the size of the semi-circular impedance shows the charge transfer resistance. There is a small arc at the nitrogen-doped graphene/ $\text{Co}(\text{OH})_2$ electrode, which indicates that the electrode material has a small charge transfer resistance. In addition, the low diffusion resistance (W) indicates that the introduction of nitrogen-doped graphene contributes to the specific surface area of the material to facilitate the transport of the electrolyte. The low charge transfer resistance and diffusion resistance indicate that the nitrogen-doped graphene composite is one of the excellent candidate materials for the supercapacitor electrode material. Meanwhile, at low frequencies, the nitrogen-doped graphene composite has a straight line that is approximately 90° . It shows that all three electrode materials have excellent capacitance performance.

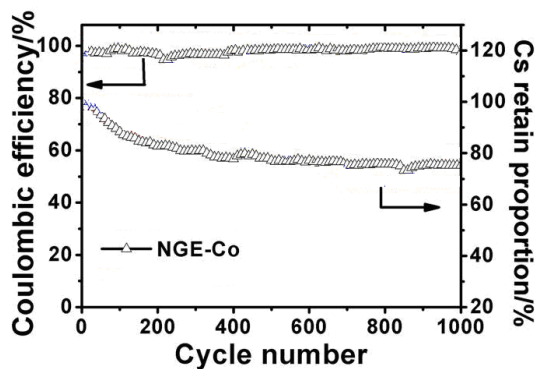


Figure 8. Cycle life curve and coulombic efficiency curve of nitrogen-doped graphene/Co(OH)₂ composites

Figure 8 is a life curve of 1000 cycles of nitrogen-doped graphene/Co(OH)₂ at a current density of 400 mA g⁻¹. It shows that after 1000 cycles, the remaining specific capacitance is 76.2% (NGE-Co), indicating that the nitrogen-doped graphene/Co(OH)₂ electrode material has good cycle performance. Meanwhile, by calculation, the Coulombic efficiency of nitrogen-doped graphene/Co(OH)₂ electrode materials is about 100%. One hundred percent Coulomb efficiency demonstrates high cycle reversibility and low energy consumption of nitrogen-doped graphene/Co(OH)₂ electrode materials. The excellent electrochemical performance of nitrogen-doped graphene/Co(OH)₂ is mainly due to the excellent electrical conductivity of nitrogen-doped graphene. During charge and discharge, the nitrogen-doped graphene can withstand the stress of volume change of Co(OH)₂, which thereby reduces the volume expansion of Co(OH)₂.

4. CONCLUSIONS

In this paper, nitrogen-doped graphene/Co(OH)₂ composites were prepared with a one-step method at moderate temperature, with graphene oxide and metal cobalt salt as precursors. It is known by characterization that the Co(OH)₂ nanowires prepared by this method were uniformly supported on the nitrogen-doped graphene sheets, and the nitrogen was successfully incorporated into the graphene. Electrochemical results show that the nitrogen-doped graphene/Co(OH)₂ composite has excellent electrochemical properties. In summary, conclusions can be drawn as follows.

1) Nitrogen-doped graphene/Co(OH)₂ nanowires (40 nm wide, 500 nm long) composite was prepared with a one-step method under moderate conditions.

2) Urea exhibits multiple functions during the synthesis process. In situ doping of graphene occurred during the reduction of graphene oxide. The slow decomposition of urea provides the desired OH⁻ for the formation of Co(OH)₂ and controls its growth rate. The excess OH⁻ and NH₃ act as soft templating agents for Co(OH)₂ to regulate its growth to obtain morphology-specific composites.

3) The electrochemical results show that as a supercapacitor electrode material, nitrogen-doped graphene/Co(OH)₂ composite material has larger specific capacitance than pure Co(OH)₂ and

graphene/Co(OH)₂. The nitrogen-doped graphene/Co(OH)₂ electrode material has low electrical resistance, good magnification characteristics, and stable cycle performance. The low-cost and fast synthesis method provides a feasible solution for obtaining supercapacitor electrode materials with excellent electrochemical performance.

References

1. M.D. Stoller, S. Park, Y. Zhu, J. An and R.S. Ruoff, *Nano Lett.*, 8(2008) 3498.
2. X.Huang, X.Y. Qi, F. Boey and H. Zhang, *Chem.Soc.Rev.*, 41(2012)666.
3. M.D. Stoller, S. Murali, N. Quarles, Y. Zhu, J.R. Potts, X. Zhu, H-W Ha and R.S. Ruoff, *Phys. Chem. Chem. Phys.*, 14(2012)3388.
4. C. Oa, Á.Caballero and J. Morales, *Nanoscale*, 4(2012)2083.
5. B. Jia and L. Zou, *Carbon*, 50(2012)2315.
6. W. Deng, X. Ji, M. Gomez-Mingot, F. Lu, Q. Chen and C.E. Banks, *Chem. Commun.*, 48(2012)2770.
7. M. Pumera, *Chem. Soc. Rev.*, 39(2010)4146.
8. P. Simon and Y. Gogotsi, *Phil. Trans. R. Soc. A*, 368(2010)3457.
9. J. Jiang, J. Liu, R. Ding, J. Zhu, Y. Li, A. Hu, X. Li and X. Huang, *ACS Appl. Mater. Inter.*, 3(2010)99.
10. Z. Lu, Z. Chang, W. Zhu and X.Sun, *Chem. Commun.*, 47(2011)9651.
11. H.J. Shin, K.K. Kim, A. Benayad, S.M. Yoon, H.K. Park, I.S. Jung, M.H. Jin, H.K. Jeong, J.M. Kim, J.Y. Choi and Y.H. Lee, *Adv. Funct. Mater.*, 19(2009)1987.
12. J. Gao, F. Liu, Y. Liu, N. Ma, Z. Wang and X.Zhang, *Chem. Mater.*, 22(2010)2213.
13. S. Stankovich, D.A. Dikin, R.D. Piner, K.A. Kohlhaas, A. Kleinhammes, Y. Jia, Y. Wu, S.B.T. Nguyen and R. S. Ruoff, *Carbon*, 45(2007)1558.
14. Z. Lei, L. Lu and X.S. Zhao, *Energ. Environ. Sci.*, 5(2012)6391.
15. H.M. Jeong, J.W. Lee, W.H. Shin, Y.J. Choi, H.J. Shin, J.K. Kang and J.W. Choi, *Nano Lett.*, 11(2011)2472.
16. Y. Qiu, X. Zhang and S. Yang, *Phys. Chem. Chem. Phys.*, 13(2011)12554.
17. H. Wang, Q. Hao, X. Yang, L. Lu and X.Wang, *Nanoscale*, 2(2010)2164.
18. H. Wang, Q. Hao, X. Yang, L. Lu and X.Wang, *ACS Appl. Mater. Interfaces*, 2(2010)821.
19. X. Fan, W. Peng, Y. Li, X. Li, S. Wang, G. Zhang and F. Zhang, *Adv. Mater.*, 20(2008)4490.
20. H. Wang, Q. Hao, X. Yang, L. Lu and X.Wang, *Electrochem. Comm.*, 11(2009)1158.
21. C. Yuan, X. Zhang, B. Gao and J. Li, *Mater. Chem. Phys.*, 101(2007)148.
22. V. Gupta, T. Kusahara, H. Toyama, S. Gupta and N. Miura, *Electrochem. Comm.*, 9(2007)2315.
23. S.R. Shieh and T.S. Duffy, *Phys. Rev. B*, 66(2002)134301.
24. J. Yang, H. Liu, W.N. Martens and R.L. Frost, *J. Phys. Chem. C*, 114(2010)111.
25. J.K. Chang, C.M. Wu and I.W. Sun, *J. Mater. Chem.*, 20(2010)3729.
26. R.S. Jayashree and P. Vishnu Kamath, *J. Mater. Chem.*, 9(1999)961.
27. L. Cao, F. Xu, Y.Y. Liang and H.L. Li, *Adv. Mater.*, 16(2004)1853.
28. H. Banda, D. Aradilla, A. Benayad, Y. Chenavier, B. Daffos, L. Dubois and F. Duclairoir, *J. Power Sources*, 360 (2017) 538.
29. H. Guo, P. Su, X. Kang, S. Ning, *J. Mat. Chem. A*, 1 (2013) 2248.
30. P. Chen, J. Yang, S. Li, Z. Wang, T. Xiao, Y. Qian and S. Yu, *Nano Energy*, 2 (2013), 249
31. C.Y. Wang, V. Mottaghitlab, C.O. Too, G.M. Spinks and G.G. Wallace, *J. Power Sources*, 163(2007)1105.
32. L. Sun, L. Wang, C. Tian, T. Tan, Y. Xie, K. Shi, M. Li and H. Fu, *RSC Adv.*, 2(2012)4498.
33. J. Li, G. Zhang, C. Fu, L. Deng, R. Sun and C. Wong, *J. Power Sources*, 345(2017) 146.

34. K. Wang, M. Xu, Y. Gu, Z. Gao, J. Liu and Q. Fan, *Nano Energy* , 31 (2017)486.
35. X. Lu, L. Li, B. Song, K. Moon, N. Hu, G. Liao, T. Shi and C. Wong, *Nano Energy*, 17 (2015) 160.
36. B. Song, J. Zhao, M. Wang, J. Mullaveya, Y. Zhu, Z. Geng, D. Chen, Y. Ding, K. Moon, M. Liu and C. Wong, *Nano Energy* ,31 (2017) 183.
37. S. Dai, Z. Liu, B. Zhao, J. Zeng, H. Hu, Q. Zhang, D. Chen, C. Qu, D. Dang and M. Liu, *J. Power Sources*, 387 (2018) 43.
38. R. Santhosh, S.R. Sita Raman, S. M. Krishna, S.S. Ravuri, V. Sandhya, S. Ghosh, N. K. Sahu, S. Punniyakoti, M. Karthik, P. Kollu, S.K. Jeong and A. N. Grace, *Electrochimica Acta*, 276 (2018) 284.
39. V. Thirumal, A. Pandurangan, R. Jayavel and R. Ilangovan, *Synthetic Metals*, 220 (2016) 524.

© 2019 The Authors. Published by ESG (www.electrochemsci.org). This article is an open access article distributed under the terms and conditions of the Creative Commons Attribution license (<http://creativecommons.org/licenses/by/4.0/>).